AD-A142 468 APPLICATION OF ELECTROCHEMICAL AND MECHANICAL IMPEDANCE MEASUREMENTS TO C.. (U) ROCKWELL INTERNATIONAL THOUSAND OAKS CA SCIENCE CENTER F B MANSFELD ET AL. MAY 84 1/1

UNCLASSIFIED SC5329.8FR N62269-82-C-0246 F/G 11/6 NL

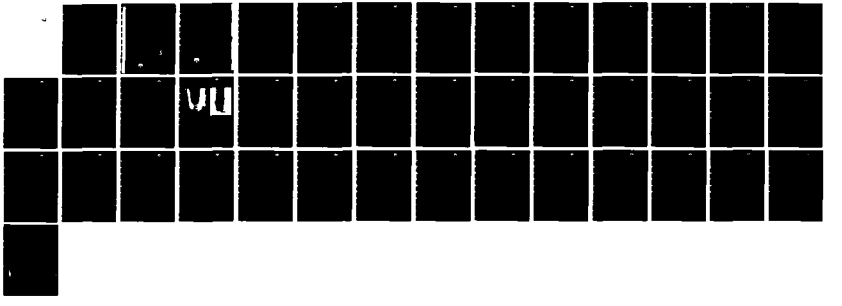

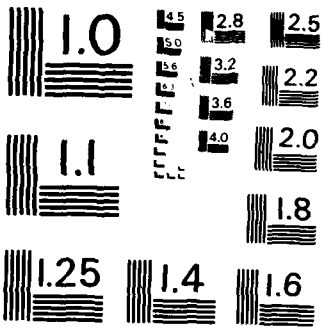

MICROCOPY RESOLUTION TEST CHART
NATIONAL BUREAU OF STANDARDS - 1963 - A

SC5329.8FR

SC5329.8FR

Copy No. 5

APPLICATION OF ELECTROCHEMICAL AND MECHANICAL IMPEDANCE MEASUREMENTS TO CORROSION INDUCED FAILURES

FINAL REPORT FOR THE PERIOD
May 24, 1982 through January 23, 1984

CONTRACT NO. N62269-82-C-0246

Prepared for

Naval Air Development Center
Warminster, PA 18974

F.B. Mansfeld and M.W. Kendig
Principal Investigators

MAY 1984

Approved for public release; distribution unlimited

Rockwell International
Science Center

Rockwell International
Science Center

... where science gets down to business

REPORT DOCUMENTATION PAGE

1a. REPORT SECURITY CLASSIFICATION Unclassified	1b. RESTRICTIVE MARKINGS
2a. SECURITY CLASSIFICATION AUTHORITY	3. DISTRIBUTION/AVAILABILITY OF REPORT Approved for public release; distribution unlimited.
2b. DECLASSIFICATION/DOWNGRADING SCHEDULE	
4. PERFORMING ORGANIZATION REPORT NUMBER(S) SC5329.8FR	5. MONITORING ORGANIZATION REPORT NUMBER(S) NADC-81309-60
6a. NAME OF PERFORMING ORGANIZATION Rockwell International Science Center 6b. OFFICE SYMBOL (If applicable)	7a. NAME OF MONITORING ORGANIZATION Naval Air Development Center
6c. ADDRESS (City, State and ZIP Code) 1049 Camino Dos Rios Thousand Oaks, California 91360	7b. ADDRESS (City, State and ZIP Code) Warminster, PA 18974
8a. NAME OF FUNDING/SPONSORING ORGANIZATION Naval Air Development Center 8b. OFFICE SYMBOL (If applicable)	9. PROCUREMENT INSTRUMENT IDENTIFICATION NUMBER Contract No. N62269-82-C-0246
8c. ADDRESS (City, State and ZIP Code) Warminster, PA 18974	10. SOURCE OF FUNDING NOS. PROGRAM ELEMENT NO. / PROJECT NO. / TASK NO. / WORK UNIT NO.
11. TITLE (Include Security Classification) (U) APPLICATION OF ELECTROCHEMICAL AND MECHANICAL IMPEDANCE MEASUREMENTS TO CORROSION INDUCED FAILURES	
12. PERSONAL AUTHOR(S) Mansfeld, Florian B. and Kendig, Martin W.	
13a. TYPE OF REPORT Final Report 13b. TIME COVERED FROM 05/24/82 TO 01/23/84	14. DATE OF REPORT (Yr., Mo., Day) MAY 1984 15. PAGE COUNT 39
16. SUPPLEMENTARY NOTATION	

17 COSATI CODES		
FIELD	GROUP	SUB. GR.

18. SUBJECT TERMS (Continue on reverse if necessary and identify by block number)
Stress corrosion cracking, corrosion fatigue, electrochemical impedance, mechanical impedance, steel, aluminum alloy.

19. ABSTRACT (Continue on reverse if necessary and identify by block number)

Measurements of the electrochemical impedance for C1117 C-Mn steel have shown that an additional, high frequency time constant occurs during straining in carbonate/bicarbonate only at potentials where stress corrosion cracking (SCC) occurs. This time constant is related to the films which are formed in the potential region where the steel undergoes SCC. Mechanical impedance measurements allow an evaluation of the extent to which applied cyclic stress couples to electrochemical reactions. For C1117 steel in phosphate (pH = 4) and carbonate/bicarbonate solutions the necessary conditions for SCC have been determined from the potential dependence of the mechanical admittance. The method is therefore useful for screening materials and environments for conditions which are necessary for SCC.

Preliminary mechanical impedance measurements have also been carried out during corrosion fatigue of Al7075-T73 in 0.5M NaCl at cathodic potentials. The ac current flowing from the cracking tip allows to evaluate the phenomena which occur in the growing crack.

20. DISTRIBUTION/AVAILABILITY OF ABSTRACT UNCLASSIFIED/UNLIMITED ☒ SAME AS RPT. ☐ DTIC USERS ☐	21. ABSTRACT SECURITY CLASSIFICATION Unclassified
22a. NAME OF RESPONSIBLE INDIVIDUAL Vinod S. Agarwala	22b TELEPHONE NUMBER (Include Area Code) (215) 441-1122 22c. OFFICE SYMBOL NAVAIR DEV CEN

DD FORM 1473, 83 APR EDITION OF 1 JAN 73 IS OBSOLETE.

TABLE OF CONTENTS

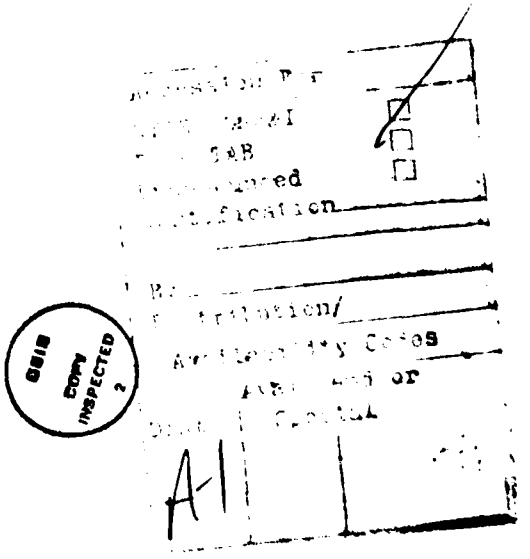

LIST OF FIGURES

LIST OF FIGURES

LIST OF TABLES

1.0 INTRODUCTION

Mechanical stress and electrochemical reactions occuring at a metal surface can interact synergistically to produce stress corrosion cracking (SCC) or corrosion fatigue (CF). Evaluation of SCC susceptibility has historically relied on placing specimens under high strain in a corrosive environment and determining the time for cracks to initiate or for load relaxation to occur. This testing includes the use of U-bends, C-rings or specimens under constant load. These tests typically require a large number of specimens which are destroyed in the course of the test. Alternatively, the reduction in strength of a test specimen pulled in tension at constant extension rate to rupture provides a rapid, but destructive test for SCC. Parkins and co-workers have employed rapid electrochemical techniques which they report to predict the potential regions at which C-Mn steels tend to crack.[1-3] Specifically, Parkins et al have determined potential regions where the steels are known to be susceptible to SCC in room temperature phosphate[2] or in carbonate/bicarbonate solutions at elevated temperatures[3] based on the difference between currents observed for rapid or slow rates of anodic potentiodynamic polarization. Armstrong and Coates[4] have obtained relaxation times for passivation from electrochemical impedance data which show characteristic features in the active-to-passive transition region where SCC was observed for low carbon steel in carbonate/bicarbonate solutions at 70°C. These empirical correlations between electrochemical results and SCC behavior were related to the interplay between dissolution and repassivation phenomena.

A better method for quantifying the synergistic relationship between mechanical stress and electrochemical kinetics could be based on measurement of currents resulting from a mechanical perturbation. Despic et al[5] have presented theoretical considerations and experimental results for the anodic currents produced by a number of metals strained elastically and plastically at different rates. They considered the current response to be the sum of electrochemical currents due to double layer charging, increased roughness,

enhanced slip edge dissolution and enhanced dissolution of the planes exposed by slip. While this work and that of others[6-8] corresponds primarily to enhanced electrode processes due to plastic deformation, Roelandt and Vereecken[9] have presented results pertaining to the electrochemical response of Alloy 600 in 1N H_2SO_4 + 0.01% KSCN under elastic conditions. They have defined a mechanical impedance as the complex ratio of applied current I_{ac}, to applied stress, $\Delta\sigma$. By analogy to the electrochemical transfer function this ratio should be defined as a mechanical admittance, Z_m^{-1}:

$$Z_m^{-1} = \frac{I_{ac}}{\Delta\sigma} \quad , \qquad (1)$$

where I_{ac} is the current responding to a mechanical fluctuation $\Delta\sigma$. Their work was performed under high anodic polarization of 0.95 and 1.0 V (SCE) and at open circuit. The phase angle vs frequency behavior of Z_m^{-1} (Eq. (1)) was related to the stability of the oxide films formed on the alloy surface. At the passive potential of 0.95 V the phase angle rapidly increased with increasing frequency between 0.16 and 1 Hz , but increased more slowly both at the onset of transpassive dissolution at 1.0 V and at the open-circuit potential. An explanation of these findings was not given. Talbot et al[10] have evaluated I_{ac} for mild steel, stainless steel and Al alloys resulting from the application of cyclic stress at 24 Hz in the elastic region in a number of electrolytes. They observed an induction time for the onset of I_{ac} for mild steel and a minimum I_{ac} at the pitting potential for the stainless steels.

In a previous project,[11] electrochemical techniques for predicting SCC susceptibility have been evaluated and constant extension rate tests (CERT) have been performed for a C-Mn steel (C1117) in 1M Na_3PO_4, pH = 4 at 21°C and in 1M $NaHCO_3$/0.1M Na_2CO_3 at 70°C at controlled potentials with continuous recording of the electrochemical impedance. The occurrence of a high frequency relaxation phenomenon in the potential region where maximum susceptibility to SCC is observed was considered as evidence that impedance

spectra can be used to assess the SCC behavior. A model for the surface reactions occurring during CERT and the resulting impedance behavior was discussed. Further work using impedance techniques was carried out initially in the present project for C1117 steel in the absence of strain for comparison with the previous data.

The main emphasis in this project was the evaluation of the electrochemical/mechanical admittance, Z_m^{-1}, defined by Eq. (1) for C-Mn steel as a function of potential in a pH 4 phosphate solution and in carbonate/bicarbonate at 70°C. Since these electrolytes produce SCC for C-Mn steel in certain narrow ranges of anodic potentials, measurements of Z_m for the steels in these environments were considered to provide a test of the usefulness of the method for evaluating SCC susceptibility. Since the mechanical stress was applied so as to remain within the elastic range, the mechanical impedance tests are essentially nondestructive.

Corrosion fatigue (CF) tests have been carried out for Al 7075-T73 in 0.5 M NaCl with the measurement of a fatigue transfer function, or fatigue impedance, defined by Eq. (2):

$$Z_k^{-1} = I_{ac}/\Delta K \qquad (2)$$

where ΔK is the cyclic stress intensity factor. Since the fatigue process involves irreversible plastic deformation at the crack tip, it cannot be described in terms of a linear response function and Z_k is not a true impedance. However, the fatigue admittance Z_k^{-1} provides a measure of the ac current responding to the applied load as normalized by ΔK. The frequency response of these very low level cyclic currents (separated from a large dc current for the bulk specimen) quantifies the extent to which the corrosion process couples to the fatigue process, thereby giving mechanistic information.

2.0 EXPERIMENTAL PROCEDURE

The experimental procedure for carrying out CERT at controlled potential with simultaneous recording of the electrochemical impedance[12] has been described in the final report of a previous project.[11] A Solartron 1174 Transfer Function Analyzer is used to obtain the electrochemical impedance data which are analyzed with a computerized system which also collects the impedance data. The approach for determining the mechanical admittance and for comparing the CF experiments will be described below.

2.1 Sample Preparation

For CERT and measurement of the mechanical admittance the specimens of C1117 steel were prepared according to the methods described in the previous report.[11] CERT experiments were performed at 70°C and 21°C in 1N carbonate/1N bicarbonate, and pH 4 1N phosphate electrolytes respectively. For the mechanical admittance tests the cell shown in Fig. 1a was used. Grips of the MTS machine clasped the threaded portion of the specimen. The teflon cell contained a Pt counter electrode and a Ag/AgCl reference electrode in a quartz Luggin capillary holder. A cyclic load of 1000 lbs amplitude was applied to the specimen to give a stress amplitude of 62 MN/m^2, not to exceed the elastic range of the material (Fig. 1b).

For the CF tests an Al 7075 double cantlever beam specimen (DCB) was machined from 1/2 in. Al 7075 plate with a T73 treatment. The TL orientation was used. The specimen had the dimensions shown in Fig. 2. The DCB specimen allows the maintainance of a constant amplitude of cyclic stress intensity as the crack grows since the stress intensity factor, K, depends only on the externally applied load,P, and sample geometry:[13]

$$K = 35.5P/\sqrt{b_n b\, w} \qquad (3)$$

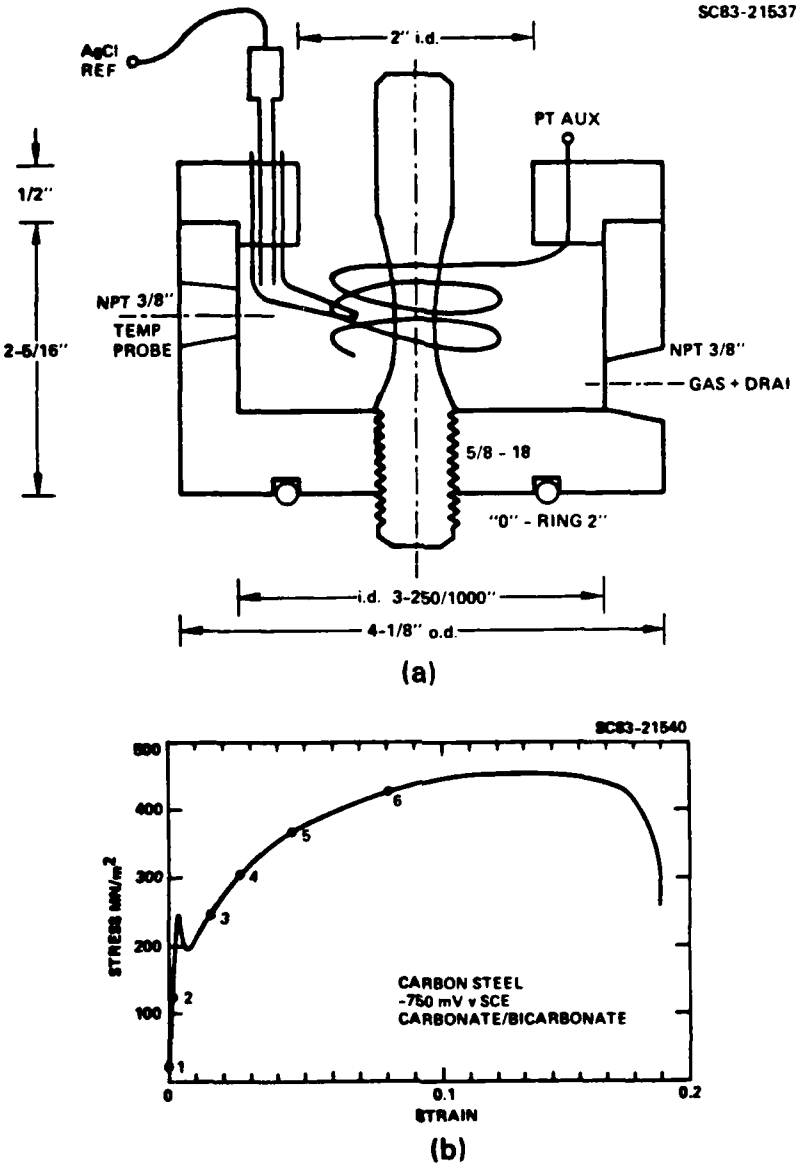

Fig. 1 (a) Cell for the mechanical impedance measurement. (b) Stress vs strain curve for C1117 steel in carbonate/bicarbonate solution at -750 mV (SCE), 70°C.

A 1.5 in. long notch was electrodischarge machined (EDM) in the specimen, the specimen was sand blasted and a scale was scribed at 25 mil intervals extending from the end of the EDM notch (Fig 2). Observation of the crack with a 3X stereo microscope allowed for the determination of the crack growth rate calculated from a least squares fit of crack length vs time data. A ΔK of

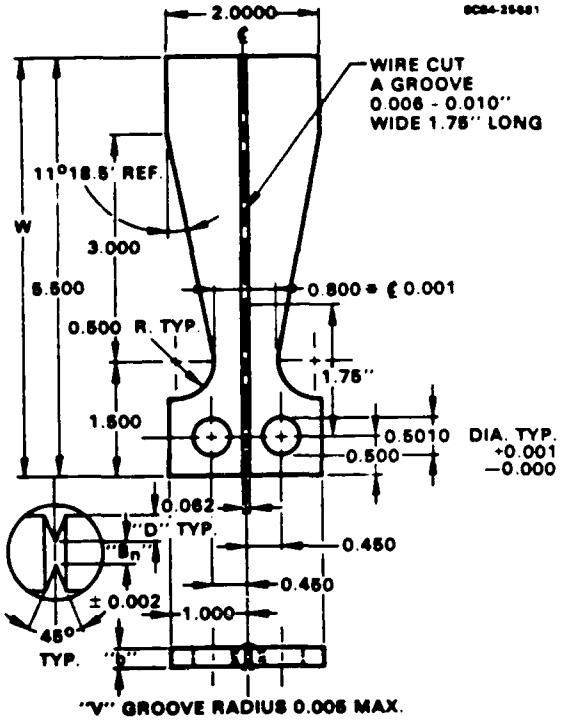

Fig. 2
DCB specimen dimensions.

350 Pa$\sqrt{m}$ with an R-ratio, K_{min}/K_{max}, of 0.27 was applied to the Al 7075-T73 TL DCB specimens in aerated 0.5 M NaCl.

Initial experiments were run with no further preparation of the Al specimen. However, a corroding region at the metal-air-electrolyte interface produced a large ac current signal synchronized with the applied load thereby dominating the ac signal from the growing fatigue crack. To eliminate this unwanted signal, the region of the specimen around the water-line was painted with a non-conducting laquer. This reduced the observed ac signal by several orders of magnitude. The remaining signal presumably results only from CF processes.

2.2 Instrumentation

The instrumentation used to detect the very small current signals, I_{ac}, synchronized with the applied loads appears in Fig. 3. The low ac signals were detected from the current response measured as a potential drop across a current measuring resistor in the case of the SCC experiments where

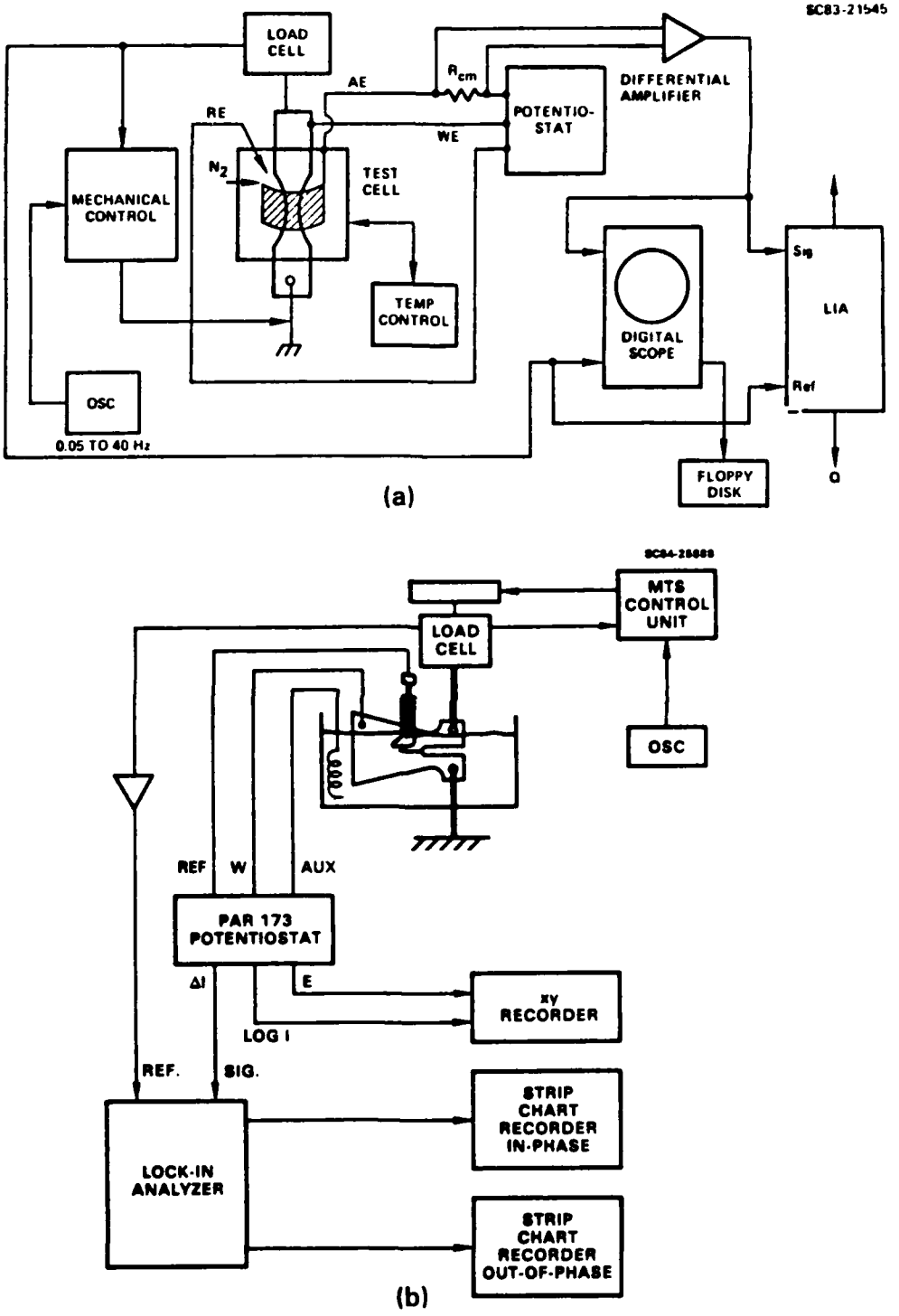

Fig. 3 (a) Schematic for the instrumentation used to obtain the mechanical impedance. (b) Schematic of instrumentation for measuring the fatigue current response.

the specimen was on a hard grou ⁴ (Fig. 3a), or from the current amplifier output of the potentiostat (Fig. 3b) for the CF experiment for which the DCB specimen was electrically isolated from the grips and therefore could be connected to the virtual ground of the current amplifier input (working electrode lead of the potentiostat). In either case the current signal was input to the signal channel of the lock-in amplifier (LIA) which was phase-loop locked to the cyclic mechanical stress either by connecting the reference of the LIA to the excitation oscillator, or directly to the load cell output through a buffer amplifier. Typically a filter with a 4 s time constant was used on the output of the LIA which gave the in-phase and out-of-phase rms I_{ac} and the rms modulus of the synchronous current, I_{ac}. The magnitude of the ac current is used as a measure of I_{ac}, which was normalized by dividing by the applied stress, to yield the mechanical admittance Z_m^{-1}, or divided by ΔK to give the fatigue admittance Z_k^{-1}. Both functions may be considered as effective mechanical-electrochemical -transfer functions (METF).

The mechanical admittance of the C1117 steel was measured as a function of potential while scanning the potential starting in the passive region (-200 to -900 mV vs Ag/AgCl in carbonate/bicarbonate solutions at 70°C, and +400 to -900 mV for the pH 4 phosphate solutions). The CF experiments were performed in 0.5M NaCl for potential scans from -1050 mV to -660 mV, while recording the LIA detected alternating current, I_{ac}. The scan rates were 1.8 mV/min.

3.0 RESULTS

3.1 Electrochemical Impedance and Stress Corrosion Cracking

In order to define more closely the potential region in which C1117 steel undergoes stress corrosion cracking (SCC), CERT was performed in 1N $NaHCO_3$ + 1N Na_2CO_3 at 70°C in the potential region between -600 mV and -750 mV vs SCE. The samples were heat treated at 970°C for one hour and furnace cooled. As Table I shows, pronounced cracking occurred at -700 mV and -750 mV. In Table I the strain ε, the yield strength Y, ultimate strength UTS, fracture energy U (as obtained by integration of the stress-strain curve) and the time-to-failure t_f are listed. Figure 4 shows the surfaces of the samples after CERT at -700 mV and -600 mV.

Table I

Summary of CERT Data for C1117 Steel in 1N $NaHCO_3$ + 1N Na_2CO_3 at 70°C

E_{appl} (mV vs SCE)	ε (%)	Y (10^6Pa)	UTS (10^6Pa)	U (N•m)	t_F (h)	Appearance	Cracks
-600	20.6	270	466	8.88	22.9	grey, dull	none
-650	21.1	200	461	8.91	23.1	black-blue	few, small
-700	18.9	199	424	7.56	20.6	brown	large
-750	19.5	200	461	8.11	21.0	black-brown	large, fine
air, RT	35.4	219	402	13.10	36.0	shiny	none

RT - Room temperature

The data in Table I, which were obtained with a slightly different electrolyte composition and different heat treatment than in the earlier work[11] to obtain increased sensitivity to SCC, confirm the earlier results, and narrow the region of susceptibility to SCC. The mechanical impedance data described below have been collected in the potential region of Table I.

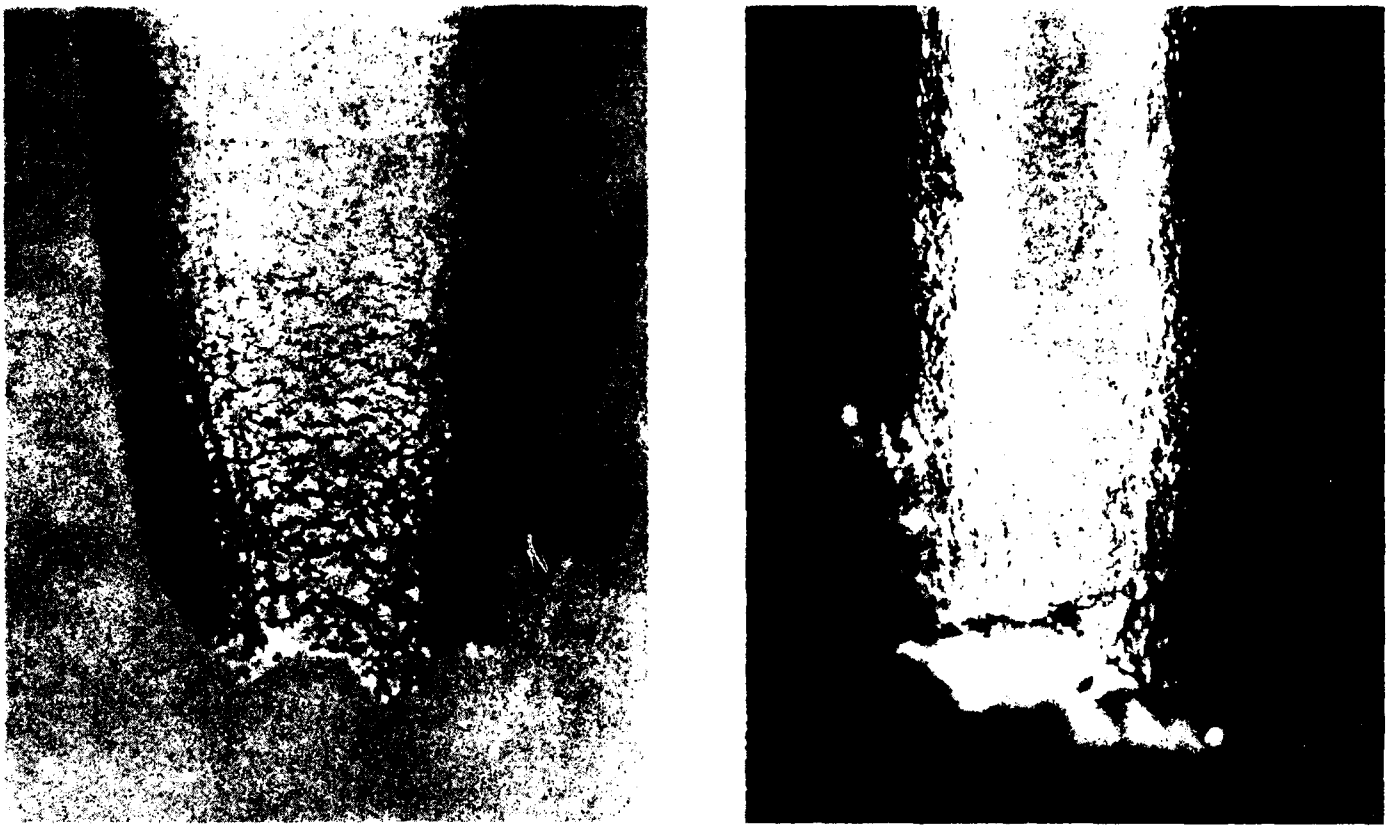

(a) (b)

Fig. 4 Appearance of C1117 steel after CERT in 1N Na_2CO_3 + 1N $NaHCO_3$, 70°C at -700 mV (Fig. 4a) and -600 mV (Fig. 4b) vs SCE.

The electrochemical impedance data (Fig. 5), which were collected during the tests of Table I confirm the earlier conclusions[11] that changes in the high frequency portion of the impedance upon transition from the elastic region to the plastic region of the stress-strain curve indicate the occurrence of SCC. At -600 mV, where SCC was not observed, no changes in the frequency dependence of the impedance $|Z|$ and phase angle θ occur during CERT. The impedance is that for a passive surface. At -650 mV, where a few, small cracks were observed, the general impedance behavior remained the same

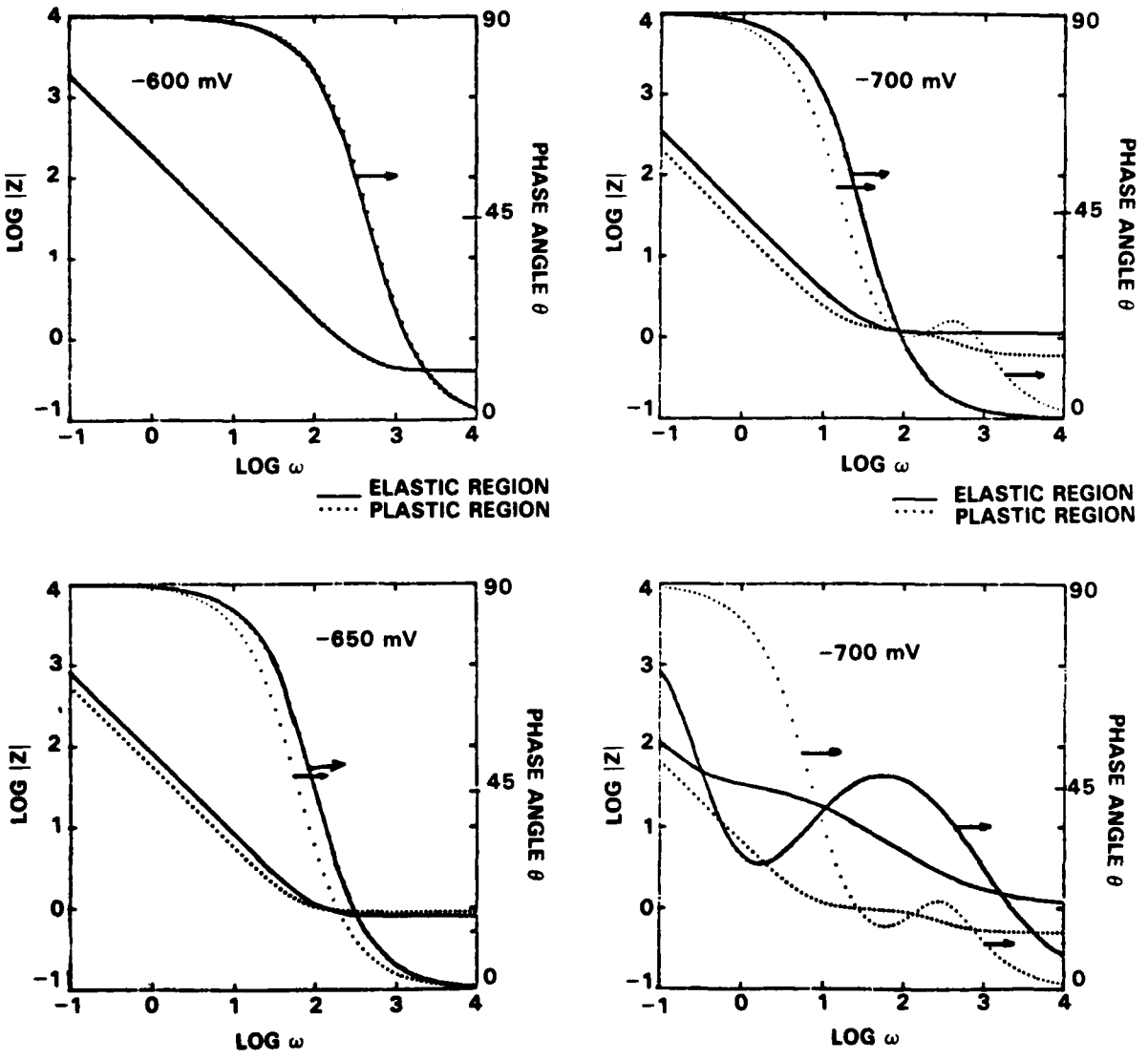

Fig. 5 Fitted impedance spectra in the elastic and plastic region for C1117 steel in 1N Na_2CO_3 + 1N $NaHCO_3$, 70°C at four potentials.

even after 0.14 cm elongation. The capacitance increased by about 45% presumably due to exposure of fresh surface. At -700 mV and -750 mV significant changes are seen. An additional time constant occurs at high frequencies during elongation, from which at -750 mV a pore resistance can be determined which decreases upon straining. The capacitance doubles upon straining.

These results are consistent with the previous conclusions that large changes in the impedance spectra upon plastic elongation at potentials where SCC occurs are due to growing cracks and rupture of surface scale. In order to determine whether these effects could be attributed directly to the elongation and consequent rupture of the surface films, impedance measurements of the same materials were made in the absence of stress as a function of time in the same potential region.

In all cases the impedance spectra (Figs. 6a-d) revealed only one apparent time constant. There were no maxima in the phase angles at high frequncies as observed at -700 mV and -750 mV for specimens undergoing elongation. In all cases the spectra could be modelled as a resistance, R_s, in series with a parallel combination of a transfer resistance, R_t, and a non-ideal impedance $(j\omega K)^{-\beta}$, where $0 \leq \beta \leq 1$. K is determined from the impedance $|Z|_1$ at $\omega = 1$ rad/s $\left(\log K = - \frac{\log|Z|_1}{\beta}\right)$. β represents the degree of deviation of the nonideal impedance $(j\omega K)^{-\beta}$ from ideal capacitive behavior for which the corresponding impedance is $(j\omega C)^{-1}$. The values of K and C are related by $C = KR_t^{\frac{1-\beta}{\beta}}$. The time constant was so low as to make the dc limit occur beyond the range of the measurement, and, hence, the values of R_t and C could not be determined. The other parameters, however, appear in Table II. At -700 and -750 mV a porous scale grows on the surface and $\beta<1$. At all potentials except -750 mV, K increases with time since a porous conducting film grows and thereby produces an increased electrode surface area. This causes a general decrease in impedance with time (Fig. 6a-c). However, at -750 mV (Fig. 6d) a decrease in K and subsequent increase in overall impedance occurs in time. Most significantly the values of R_s, which is the sum of solution resistance plus film resistance, show little or no change with time for all potentials.

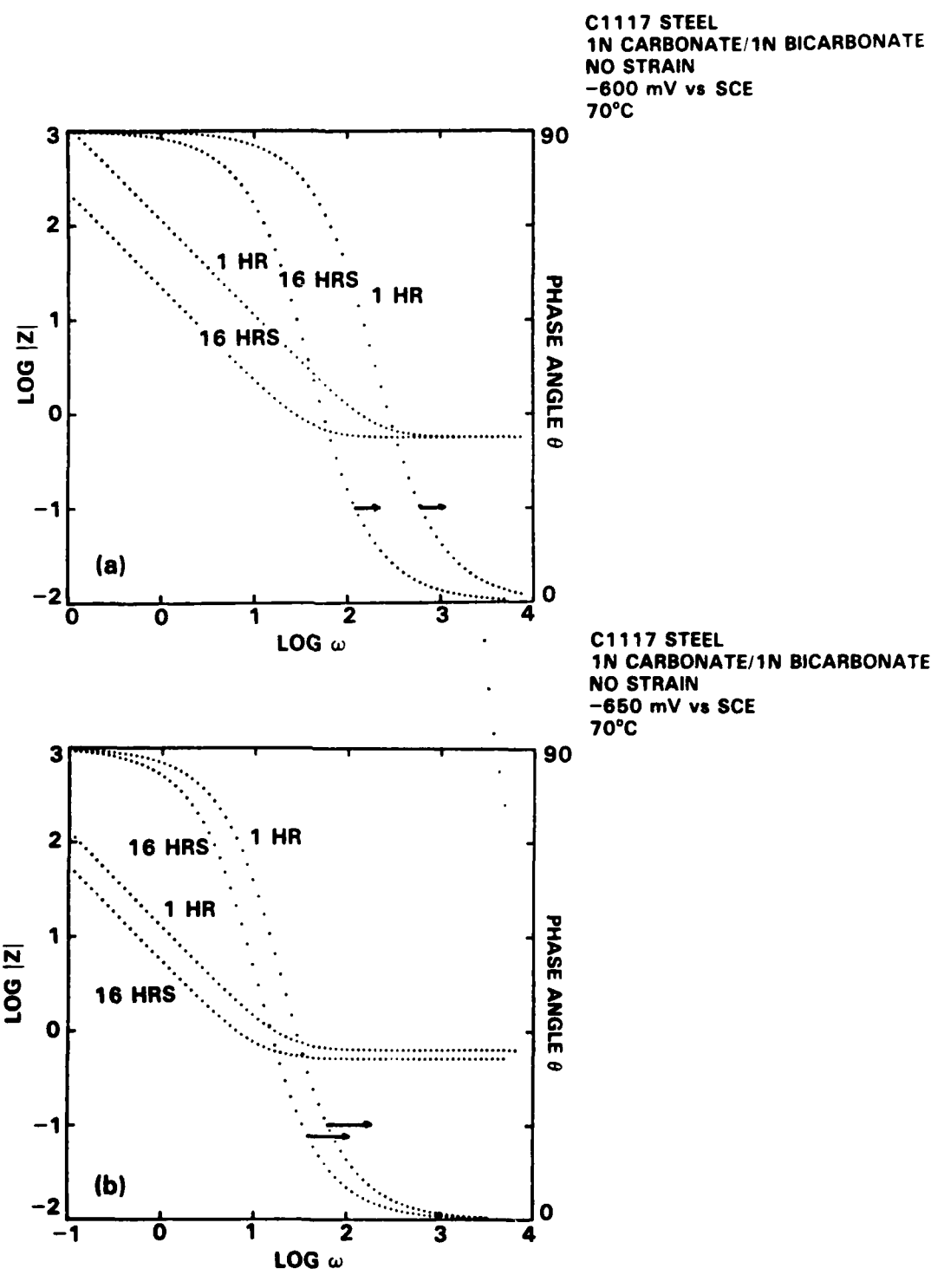

Fig. 6a-b Electrochemical impedance of C1117 steel in 1N Na_2CO_3 + 1N $NaHCO_3$ after 1 h and 14 or 16 h at four different potentials.

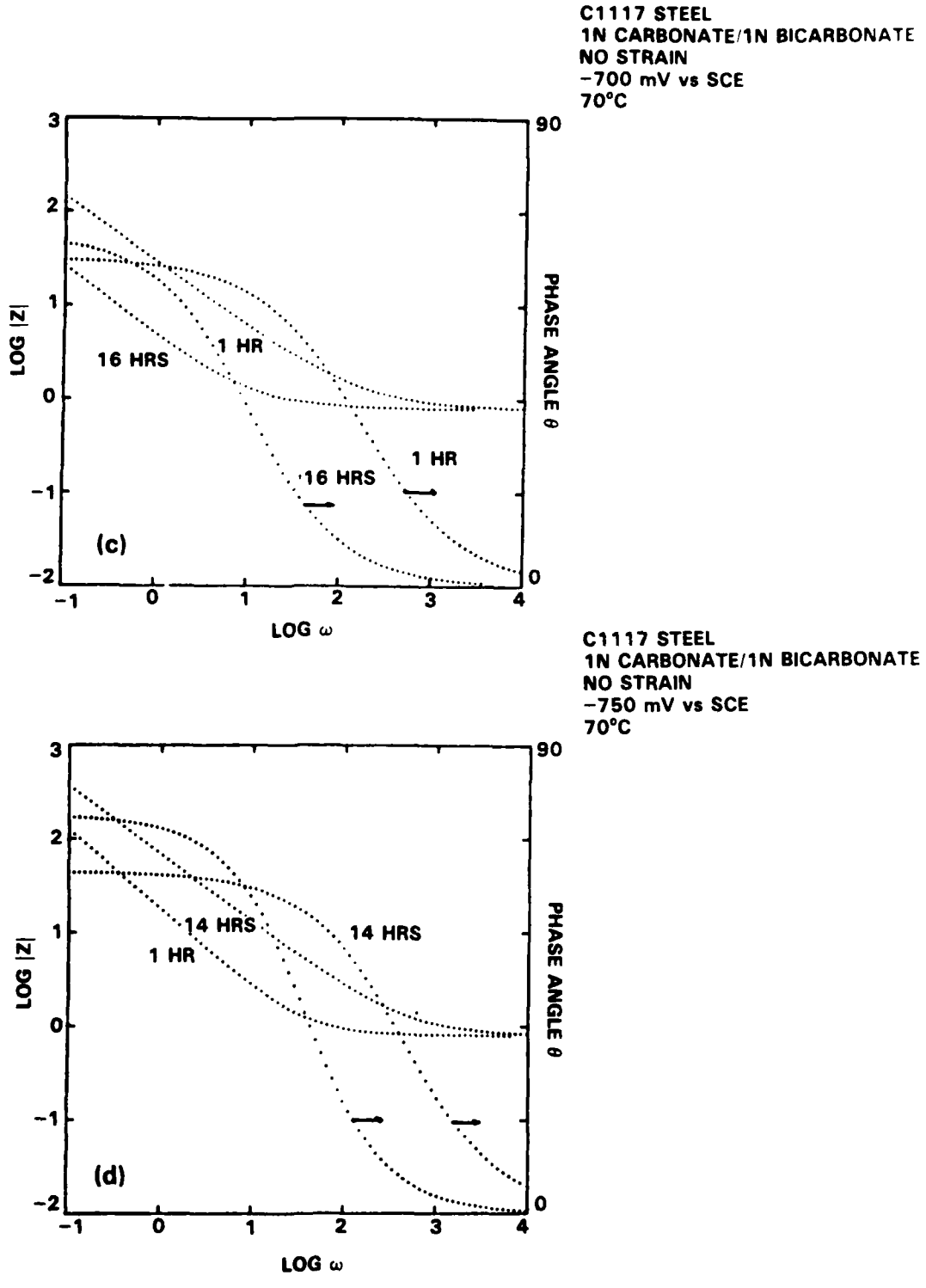

Fig. 6c-d Electrochemical impedance of C1117 steel in 1N Na_2CO_3 + 1N $NaHCO_3$ after 1 h and 14 or 16 h at four different potentials.

Table II

Analysis of Impedance Data for Unstressed C1117 Steel at 1h and 12-16h in the Absence of Applied Stress (Fig. 6a-d)

E_{appl} (mV vs SCE)	1h R_s (ohm)	1h K $(F^{1/\beta} \cdot s^{(1-1/\beta)})$	1h β	12-16h R_s (ohm)	12-16h K $(F^{1/\beta} \cdot s^{(1-1/\beta)})$	12-16h β
-600	0.6	$8.9 \cdot 10^{-3}$	1.0	0.6	$4.5 \cdot 10^{-2}$	1.0
-650	0.6	$7.8 \cdot 10^{-2}$	1.0	0.5	$1.8 \cdot 10^{-1}$	1.0
-700	0.8	$8.2 \cdot 10^{-3}$	0.70	0.8	$1.3 \cdot 10^{-1}$	0.75
-750	0.8	$3.4 \cdot 10^{-2}$	0.85	0.8	$3.0 \cdot 10^{-3}$	0.73

F = farad

This contrasts to the case described previously where the specimens undergo strain and show rather significant changes in R_s with time at -700 mV and -750 mV.

Table III summarizes the ratios R_s^i/R_s^f between the impedances as a function of time or R_s^e/R_s^p as a function of strain as observed previously. Under strain, changes occur in the surface films which cause R_s^p in the plastic region to decrease giving rise to ratios of R_s^p/R_s^e significantly greater than 1, which can be considered as a diagnostic criterion for the occurrence of SCC.

Despite the fact that a time dependence for the growth or loss of surface films appears for the unstressed samples, no additional time constants N_τ become apparent during the 12-16 hour period of observation, while two time constants occur in the region of SCC (Table III). Most significantly no decrease in the resistance of the surface films occurs as a function of time for the unstressed specimens, the ratios of the initial to final values R_s^i/R_s^f are all near 1.

These results show that the susceptibility to SCC can be determined from the analysis of impedance data obtained during CERT. The number of time constants and the related changes of the resistance of surface films can serve

as diagnostic criteria. Only one time constant appears in the impedance spectrum at all potentials even after the 12-16 hour exposure for C1117 specimens in the absence of strain. However, during CERT two time constants occur at -700 mV and -750 mV (see Table III). In the absence of strain, no decrease in the series resistance occurs, which is not the case for the strained surface, where significant changes occur. Significantly, Parkins[1] has pointed out that SCC is observed only at potentials where a particular surface film is formed.

Table III

Comparison of Time Constants and Series Resistances for Stressed and Unstressed C1117 Steel in 1N Na_2CO_3 + 1N $NaHCO_3$ at 70°C

E_{appl} (mV vs SCE)	Unstressed			Stressed (CERT)		
	N_τ^i	N_τ^f	R_s^i/R_s^f	N_τ^e	N_τ^p	R_s^e/R_s^p
-600	1	1	1.0	1	1	1.0
-650	1	1	1.2	1	1	0.9
-700	1	1	1.0	1	2	1.9
-750	1	1	1.0	2	2	2.2

N_τ: Number of time constants: elastic region (e), plastic (p); initial (i), final (f).

R_s^e/R_s^p: Ratio of series resistance observed during elastic deformation to series resistance observed during plastic deformation.

R_s^i/R_s^f: Ratio of series resistance observed at initial exposure times to the series resistance observed at 12-16 hrs.

3.2 The Relationship Between SCC Susceptibility of C1117 Steel and The Mechanical Admittance

Figure 7 presents the measured mechanical admittance for the C1117 steel in the carbonate/bicarbonate solution at 70°C. Maxima of I_{ac} and

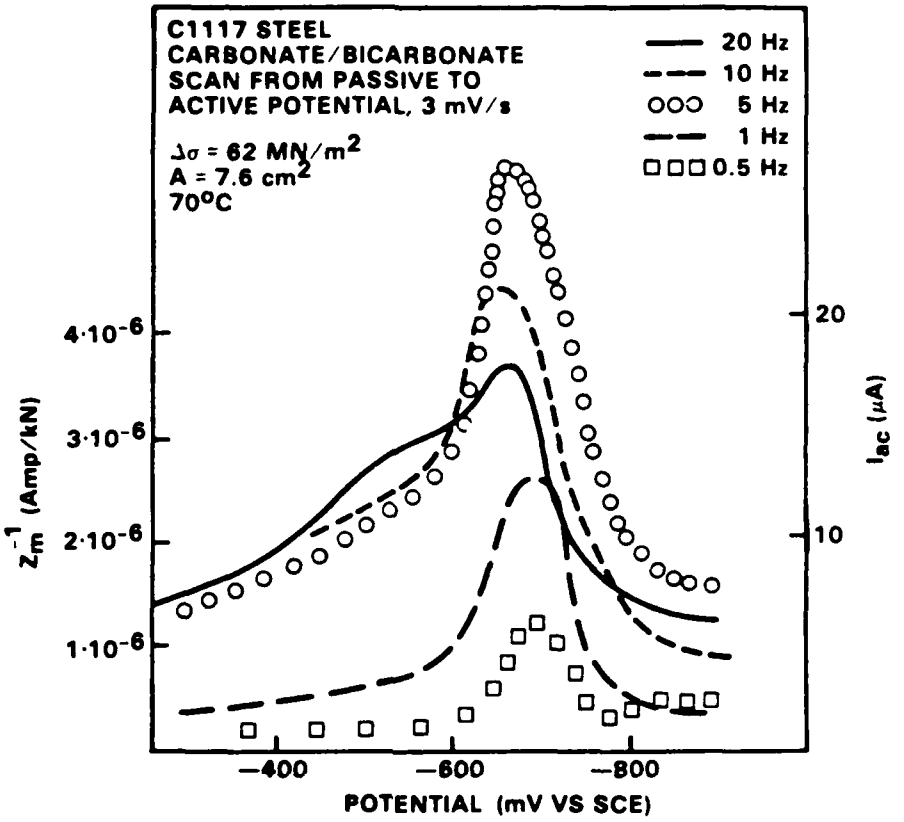

Fig. 7 Response, I_{ac}, to the cyclic stress, $\Delta\sigma$ = 63 MN/m^2 and mechanical admittance Z_m^{-1} as a function of frequency of applied load.

Z_m^{-1} synchronized with applied stress appear in the region between -650 and -750 mV. The specific mechanical admittance Z_m^{-1} may be defined as:

$$Z_m^{-1} = \frac{i_{ac}\, a_x}{P} \quad , \tag{4}$$

where P is the applied load fluctuation, a_x the cross sectional area of the specimen's gauge section and i_{ac} the alternating current density. For a gauge section of exposed surface area a_s:

$$Z_m^{-1} = \frac{a_x}{a_s} \frac{I_{ac}}{P} \quad , \tag{5}$$

where I_{ac} is the observed ac current. An exposed surface of the 0.95 cm (3/8 in.) × 2.54 cm (1 in.) gauge section has an area as = 7.6 cm^2 and a cross sectional area a_x = 0.71 cm^2. A load amplitude of 1000 pounds gives P/a_x = 63 MN/m^2. The left axes in Figs. 7, 9 and 10 contain the mechanical admittance values, Z_m^{-1}, corresponding to the observed I_{ac} shown on the right axes of the figures. The values of Z_m^{-1} lie considerably above the values calculated for the charging of the double layer of 3.6×10^{-9} amp/kN as calculated previously.[11]

The magnitude of the maximum I_{ac} (or Z_m^{-1}) in Fig. 7 depends on the frequency of the applied load. A current value determined by subtracting the baseline value of I_{ac} from the maximum I_{ac} represents an intensity of the current response for a given frequency, which is plotted in Fig 8. The frequency dependence of the intensity, I_{ac}^{max}, for the coupling of the stress to the electrochemical reactions takes the form of an S-shaped curve. At low frequencies corresponding to low strain rates, I_{ac}^{max} is low, whereas at high frequencies I_{ac}^{max} reaches a new plateau. This could be explained by more rapid degradation than passivation of the surface film at high frequencies, while at low frequencies the repassivation reaction heals the film as soon as it degrades by rupture or thinning. It should be noted that for 5 Hz and above, enhanced I_{ac} exists even at potentials above -650 mV (Fig. 7) showing that high strain rates cause a coupling of electrochemical reactions to stress well into the passive region.

Figure 9 shows both the alternating current, I_{ac}, and the dc current, I_{dc}, for the C1117 steel in pH 4 phosphate for a cathodic potentiodynamic scan from a passive potential of 400 mV to -900 mV vs SCE at a frequency of 5 Hz of the applied load. There appears to be some correlation of I_{ac} with I_{dc}, but only for anodic currents. No coupling with the cathodic reaction occurs as

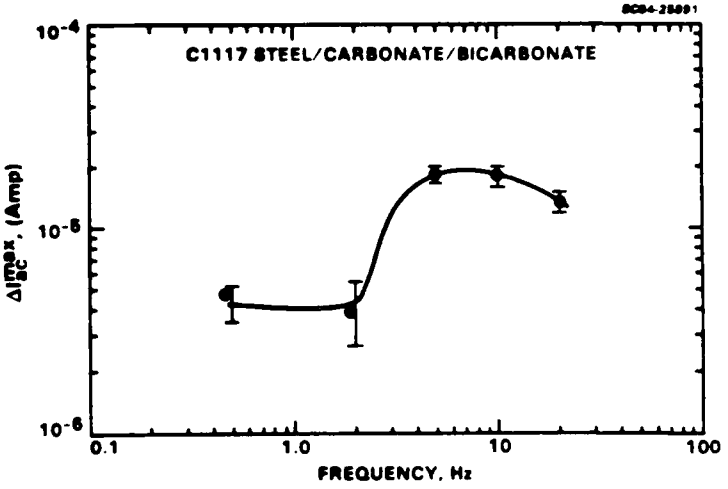

Fig. 8
Dependence of maximum minus baseline I_{ac} from Fig. 7 on the frequency of applied stress.

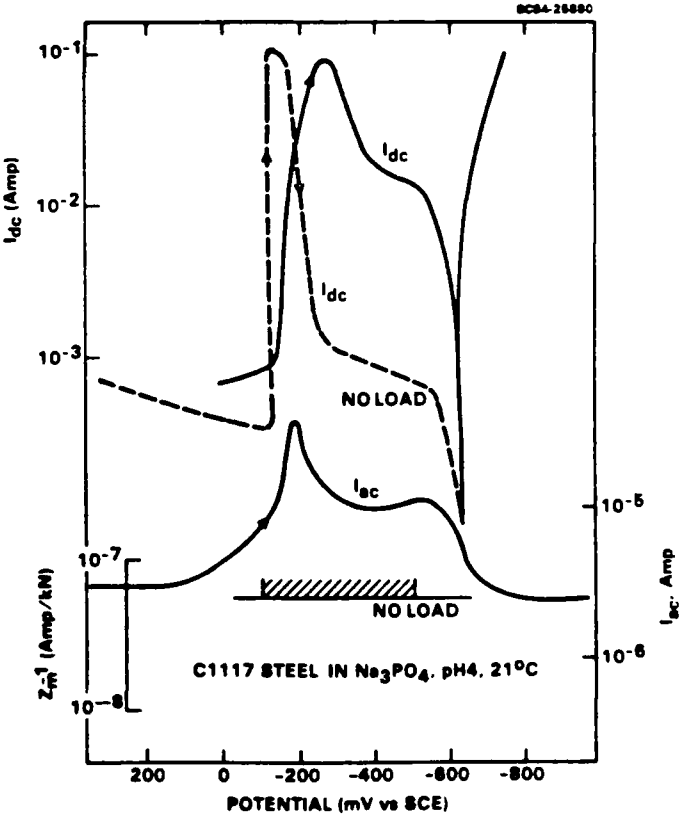

Fig. 9
Z_m^{-1}, I_{ac} and I_{dc} for C1117 steel in 1N Na_3PO_4, pH 4, 21°C for a potential scan from passive to active potentials at a rate of 30 mV/min.

cathodic as -900 mV. In the absence of load, no ac current above the baseline value appears, but a large maximum of I_{dc} corresponding to reactivation on the scan from the passive to the active region appears at -150 mV which is more noble than the corresponding current peak in the presence of a cylic load. The corresponding results for an anodic scan from -800 mV to 400 mV appear in Fig. 10. As for the cathodic scan a coupling of current to the mechanical events exists only at anodic potentials as evidenced by the presence of only baseline I_{ac} at cathodic potentials. Two current peaks of the anodic ac response appear which correlate roughly with the maxima of the dc current, I_{dc}. Some oscillations in I_{dc} appear at about -150 mV (Fig. 10), where the second maximum of I_{ac} occurs.

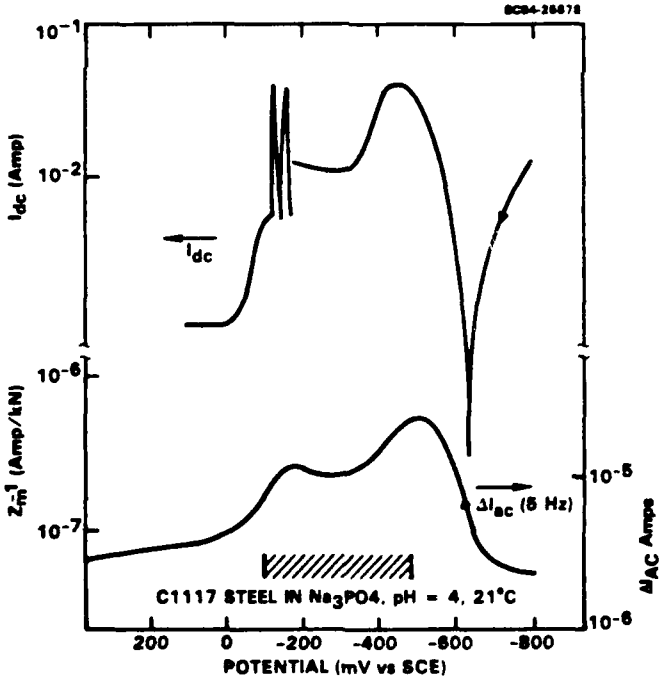

Fig. 10 Z_m^{-1}, I_{ac} and I_{dc} for C1117 steel in 1N Na_3PO_4, pH 4, 21°C for a potential scan from active to passive at a rate of 30 mV/min.

A comparison of I_{ac} (and Z_m^{-1}) at 20 Hz and 5 Hz in Fig. 11 shows some differences in the potential dependence for a cathodic scan. At 20 Hz a significant ac response occurs at passive potentials above -100 mV. Apparently the higher strain rates occurring at the higher frequencies of applied load tend to extend the range for the coupling of anodic electrochemical processes to mechanical stress to more anodic potentials as in the carbonate/bicarbonate case (Fig. 7). Significantly no coupling of electrode kinetics to cathodic reactions occurred in the cathodic region, as was also observed in the case of the carbonate/bicarbonate environment.

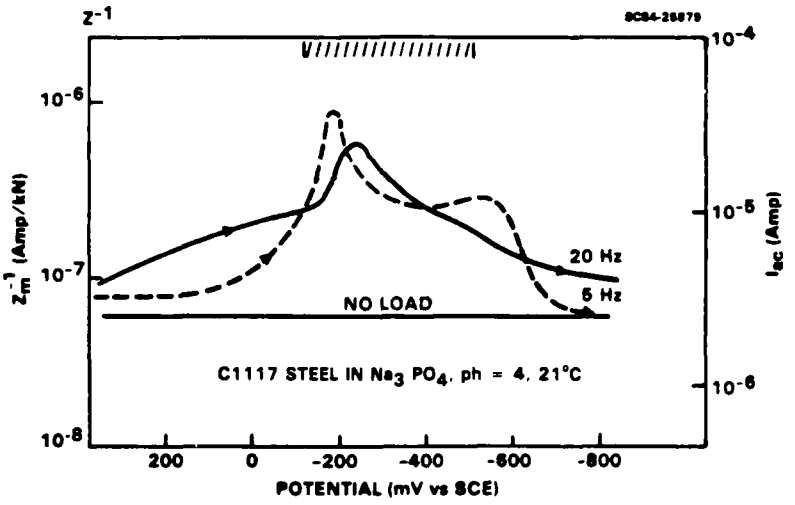

Fig. 11 Potential dependence of I_{ac} at 5 Hz and 20 Hz for the C1117 steel in pH 4 phosphate solution.

Table IV shows some results for the constant extension rate tests (CERT) for the C1117 steel in the pH 4 phosphate solution. Although there is some evidence for weakening at -525 mV which corresponds to the maximum of I_{ac} at 5 Hz (Fig. 11), no cracks were observed at any of these potentials from

microscopic examination. Parkins et al[2] have observed SCC for carbon-manganese steels in pH 4 phosphate between -100 mV and -480 mV (SCE) with a sharp maximum in the cracking rate at -175 to -200 mV. Parkins' data should, however, be considered with caution, since it was claimed that SCC occurs only in 1M Na_3PO_4 and 1M Na_2HPO_4, but not in 1M NaH_2PO_4, which from a chemical standpoint is surprising since at pH 4 the actual solution components will be the same for all of these solutions. Our previous electrochemical studies in these solutions had indeed not shown any differences in the anodic potentiostatic curves.[11]

Table IV

Summary of CERT Data for C1117 Steel in 1N Phosphate at pH 4

E_{appl}	Y (10^6 Pa)	UTS (10^6 Pa)	U N•m
-525	224	356	10.1
-225	281	427	13.8
+300	272	452	14.7
Air	219	402	13.1

A comparison of the CERT data in Tables III and IV and the mechanical admittance results demonstrates that the current response synchronized with applied mechanical stress shows whether or not mechanical stress in the elastic region couples to electrochemical reactions. These measurements define the necessary conditions for SCC, but perhaps not the sufficient conditions. The method can therefore be used as a tool for rapidly drawing the environmental domains (defined by either elecrochemical or chemical potential) where SCC might occur for a given material. The susceptility to SCC can then be defined by a few additional constant extension rate tests in the region where a mechanical admittance was detected, while in the conventional approach a large test matrix is needed to determine the potential regions for SCC susceptibility.

3.3 Coupling of Electrochemical Processes to the Corrosion Fatigue of Al 7075-T73

Figure 12 shows the observed crack growth rate for A17075-T73 at a stress intensity factor of 350 Pa$\sqrt{m}$ and R-ratio of 0.27 in 0.5 M NaCl. The growth rate shows a tendency to increase with the frequency of the cyclic load and potential as expected for materials exhibiting dissolution enhanced CF.[14]

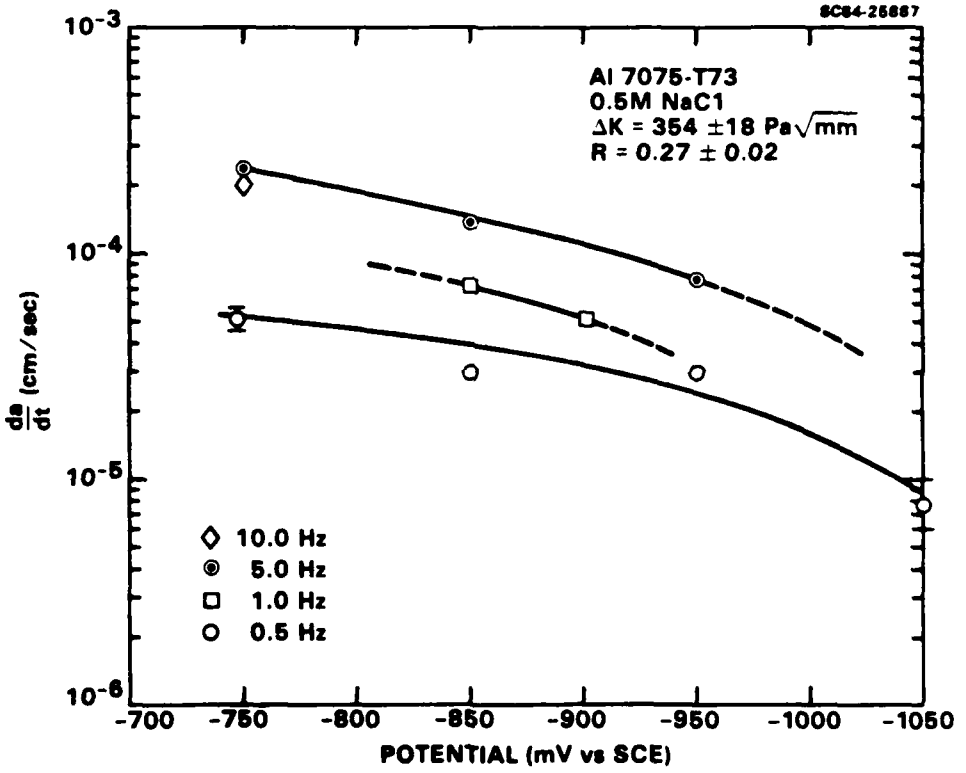

Fig. 12 Crack growth rate as a function of potential and frequency for cyclic stress intensity factor, ΔK = 350 Pa$\sqrt{m}$, and R-ratio = 0.27.

Using the apparatus shown in Fig. 3b, the ac current responding to the cyclic load was measured. The ac current response, I_{ac}, divided by ΔK defines the effective fatigue admittance, Z_k^{-1} (Eq. (2)). Since the response is not linear, Z_k^{-1} does not represent a true transfer function. Nevertheless,

the function as defined in Eq. (2) provides a measure of the coupling of the cyclic load to the electrode kinetics in the growing crack. Initial experiments showed ac currents between 0.01 and 1 μa. However, it was realized that corrosion at the air/electrolyte/metal interface was responsible for this response as a result of the modulation of the waterline position of the sample due to the slight deflection of the specimen above and below the electrolyte/air interface. Waterline corrosion of the specimen was eliminated by painting the portion of the specimen that exists at the electrolyte/air interface with a non-conducting polymeric masking material. As a result, the observed ac response decreased by several orders of magnitude, but could still be measured.

The results for the ac response expressed as Z_k^{-1}, and the dc current, I_{dc}, are presented in Fig. 13 as a function of potential for several frequencies. Several important observations can be made concerning the data in Fig. 13. First, the cathodic dc current shows a plateau around -900 mV which corresponds to the diffusion limited current for oxygen reduction and relates to the hydrodynamic conditions at the electrolyte/metal interface of the bulk specimen due to the slight agitation of the sample with the cyclic load. A plot of the plateau I_{dc} vs the root of the frequency, $\sqrt{f}$, shows the expected linear relationship (Fig. 14). The ac response provides information related to the electrochemical kinetics in the crack tip. The minimum of I_{ac} vs applied potential in Fig. 13 represents the point where applied cyclic load results in the least change in current and presumably occurs at the position of the open circuit potential for the crack tip, E_o^c. Minima in the ac response of fatigued stainless steel have been observed at applied anodic potentials and related to the pitting and breakdown potentials.[10]

The fact that the ac current, as represented by Z_k^{-1} in Fig. 13, does not actually go to zero may be due to the fact that some ac current will always flow in the crack as a result of the charging of the double layer and as a result of forming and eliminating surfaces produced by the emerging slip steps despite the fact that no net faradaic current flows. It is significant, however, that the effective corrosion potential E_o^c of the new surface formed

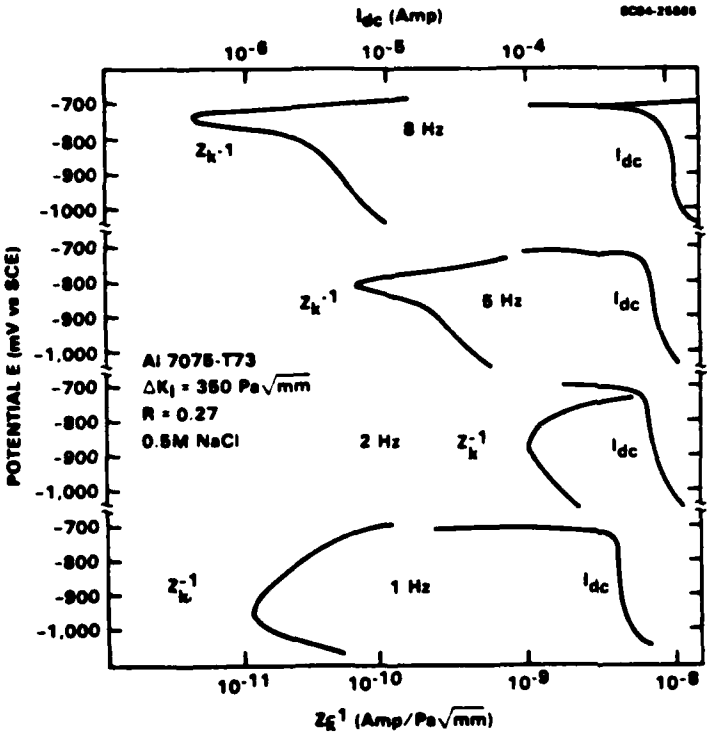

Fig. 13
Z_k^{-1} and I_{dc} for Al 7075-T73 DCB-TL specimen as a function of potential and frequency of applied ΔK.

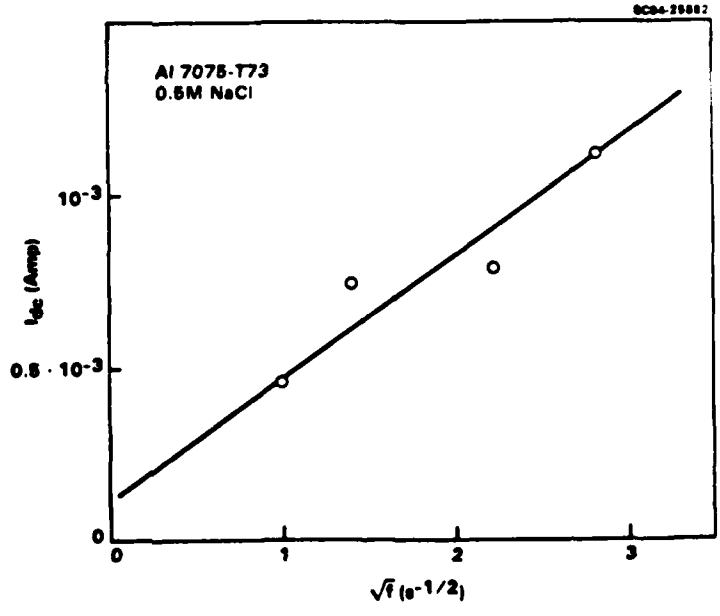

Fig. 14
Plateau value of I_{dc} vs $\sqrt{f}$.

at the crack tip can be evaluated using this technique. As indicated in Fig. 13 and plotted in Fig. 15, the difference between open circuit potential of the bulk material, E_o, and that of the crack tip, E_o^c, decreases with applied frequency. At 1 Hz, E_o^c shifts more than 200 mV in the active direction(toward negative potentials), while at 8 Hz the shift is only 30 mV.

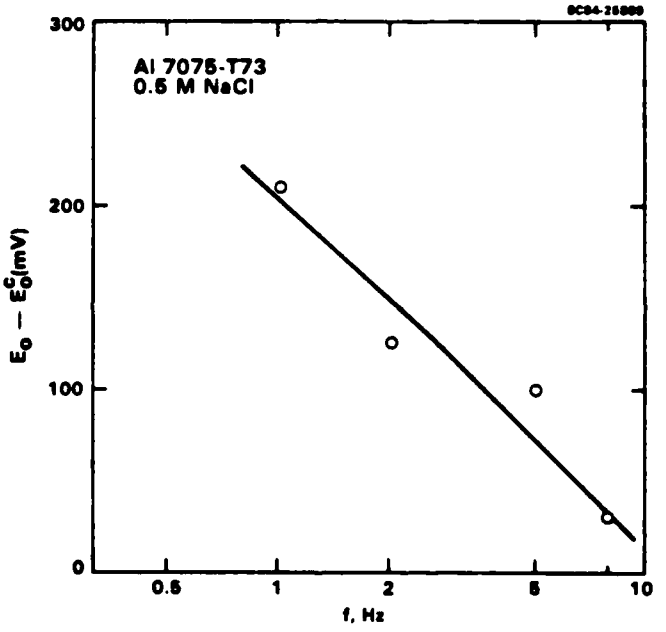

Fig. 15 The difference between the open circuit potential E_o of the bulk Al 7075 and the crack tip E_o^c as a function of the frequency of the modulation of ΔK.

The frequency dependence of the corrosion processes in the crack tip may also be illustrated in Fig. 16 which shows the crack growth rates at -750 mV in terms of both da/dt and da/dN, and the fatigue admittance, Z_k^{-1}, for -750 mV and $Z_{k,o}^{-1}$ estimated for E_o^c. The crack growth rates show the type of frequency dependence typical of dissolution controlled processes activated by plastic strain in the crack tip region.[14] The ac response as represented by

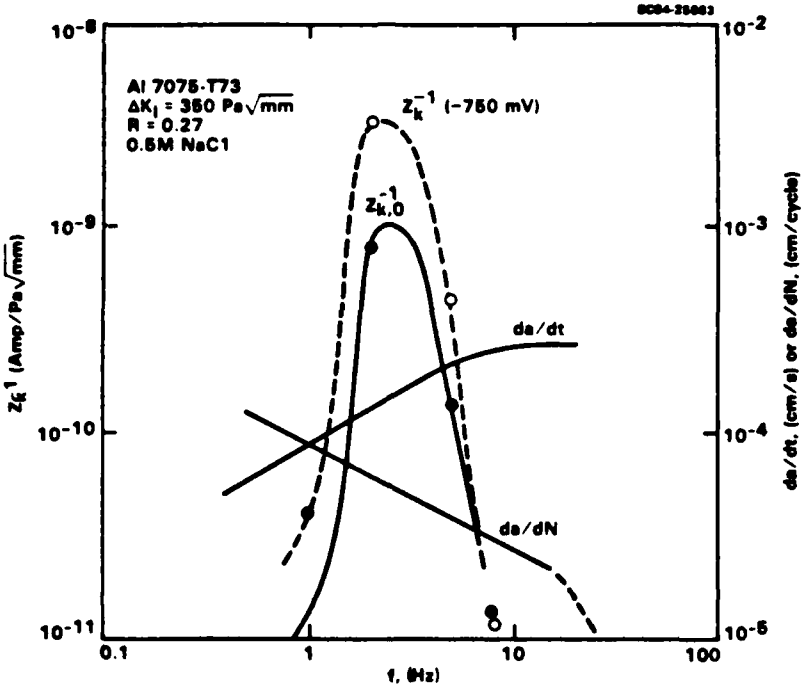

Fig. 16 Fatigue admittance Z_k^{-1} and crack growth rates as a function of frequency.

the fatigue admittance shows a maximum with respect to frequency. This apparent resonance effect is believed to result from the tuning of the cyclic modulation of K to the kinetics of the corrosion process as illustrated in Figs. 17a and b.

Upon loading the fatigue cracked specimen, slip steps emerge at the crack tip, and, after a short induction time, a rapid dissolution process occurs as a result of anodic attack of the emerged slip steps. This process, however, is self limiting and after a sufficient time the local dissolution of the new surface stops when the active surface of the slip steps has been consumed and the current falls. Figure 17a schematically shows this mechanism. As a result, the rms ac current response will be optimized where the

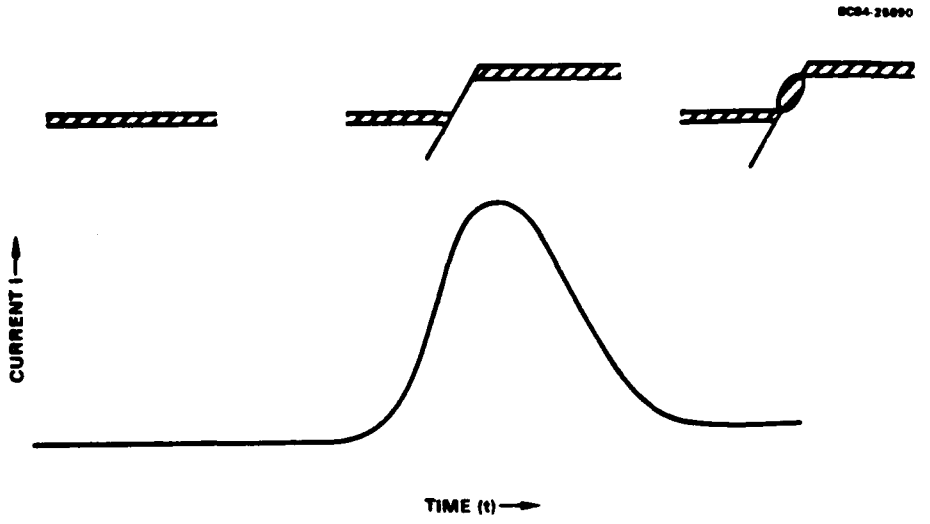

Fig. 17a Schematic of the electrochemical dissolution of emerging slip steps.

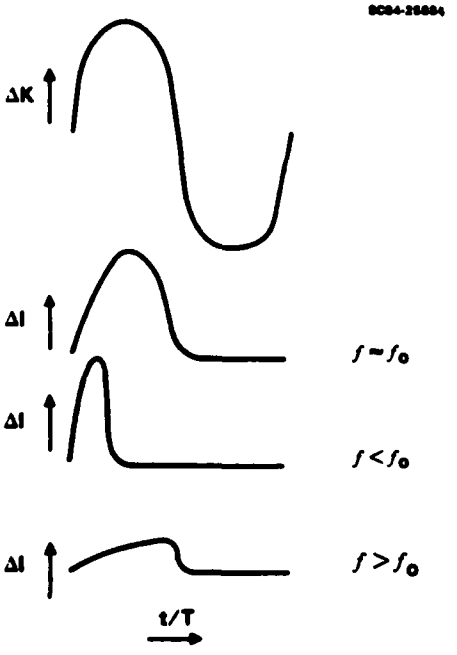

Fig. 17b
Schematic of the electrochemical-mechanical resonance resulting from slip step dissolution kinetics.

characteristic time for the metal dissolution equals one half of the load cycle as shown in Fig. 17b. This explains the occurrence of the maximum Z_k^{-1} in Fig 16. The characteristic time for the slip step dissolution/ oxidation is therefore 0.2 s at -750 mV in 0.5 M NaCl.

The extent of dissolution that occurs in a cycle that contributes to CF can be estimated by considering the observed ac current of 0.35 μamp at the corrosion potential E_o^c of the crack tip for 2.5 Hz. This corresponds to a charge of 0.28 μcoul per cycle or conversion of a volume of 10^{-11} cm^3 of Al metal to Al(III) compounds. Alternatively, the current density responsible for the CF component of the fatigue can be determined as 3 A/cm^2 assuming the CF component of the crack rate is 10^{-4} cm/s (Fig. 16). Using the observed currents of 0.35 μA, this implies that an area of 1.1×10^{-7} cm^2 represents the critical portion in the crack where corrosion occurs. Certainly this is a small area, but it is consistent with the observation made by Duquette and Uhlig[15] that removal of the equivalent of 10^{-4} atom layer/cycle could explain the CF behavior in steel. The important point is that enhanced dissolution/ oxidation of active sites on an atomic scale (e.g. slip bands) can be efficiently directed by the fatigue process into enhanced crack growth.

These initial results show that a wealth of information can be obtained using a technique which scrutinizes the electrochemical kinetics of the crack tip during fatigue. Further work needs to be done to quantify the technique to extend it to other systems of potential importance.

4.0 SUMMARY

The results presented here show that the electrochemical impedance and the mechanical admittance techniques can evaluate whether necessary conditions exist for SCC since they provide sensitive measures of the coupling of electrochemical processes to applied mechanical stress. Both tests can be used to detect regions of potential, metallurgical conditions or environmental compositions where SCC could occur. Confirmation of the susceptibility to SCC would require some further mechanical tests. Measurements of the mechanical admittance provide information concerning the mechanical properties of protective films which are lacking at present, but are very much needed to understand SCC of passive systems.

The effective fatigue admittance provides a method for evaluating the electrochemical properties and kinetics that occur at the crack tip. This method provides useful insights into the mechanistic aspects of CF. The results for the CF of Al 7075-T73 in 0.5 M NaCl show that dissolution or oxidation of emerging slip steps,although representing a small extent of corrosion, significantly enhances the fatigue rate.

All of the measurements described here provide preliminary data for the use of new techniques which by design are highly selective to those electrochemical reactions which result from applied stress. The mechanical admittance test should be applied to other systems exhibiting SCC in a narrow potential or composition range in order to gain further confidence in the approach. As for the fatigue admittance, additional data should be obtained for the fatigue of the Al 7075 system. Methods for enhancing the S/N resolution of the measurement must be obtained and data for wider ranges of crack growth rate, ΔK,frequency, potential and pH for a variety of alloy/environmental conditions need to be obtained in order to conclusively evaluate the validity of the approach.

5.0 RECOMMENDED USE OF THE IMPEDANCE TECHNIQUES

Electrochemical impedance techniques have been found to be useful for evaluation of the electrical properties of films formed on carbon steel surfaces in carbonate/bicarbonate solutions and pH 4 phosphate solutions. When an applied stress ruptures these films, changes in the electrical properties as determined from the electrochemical impedance spectra have been shown to occur. Electrochemical impedance can, therefore, evaluate the integrity of surface films under the conditions of corrosion and stress without polarizing the metallic surface. The method can best be used in laboratory testing for evaluating the relative stability of surface films under conditions related to SCC.

Mechanical impedance methods enable an evaluation of the extent to which applied cyclic stress couples to electrochemical reactions. For C1117 steel in phosphate (pH 4) and carbonate/bicarbonate solutions the increase of the mechanical admittance above the baseline indicates the necessary conditions for SCC. Furthermore, the test is nondestructive in that the amplitude of the applied cycle stress does not exceed the elastic limit of the bulk material. Use of the method for screening materials and environments for the presence of conditions necessary for SCC is recommended. It defines a smaller number of additional CERT tests that would have to be performed to actually confirm that sufficient conditions for SCC are present and SCC actually occurs. The mechanical impedance method shows promise as a tool for simplifying the process of evaluating materials and environments for SCC susceptibility. The application of the mechanical admittance method to CF allows the study of crack tip phenomena. This method needs to be applied to a large variety of metal/environment systems for comparison of kinetics and mechanisms of CF.

6.0 RECOMMENDED FUTURE RESEARCH

The work performed under this project can be considered as an initial effort to adapt electrochemical impedance techniques, which have been found to be very useful for the evaluation of corrosion inhibition by inhibitors and coatings,[12] to the evaluation of SCC and CF. Some questions concerning the mechanical impedance technique remain at this point. Talbot et al[10] have observed different levels of alternating current responding to the cyclic reverse bending of a carbon steel specimen in alkaline and neutral electrolytes as a function of time. Are induction times necessary, or does the system require a certain time for films to develop before an enhanced mechanical admittance occurs in the susceptible region? Measurement of the time dependence of the mechanical admittance of C1117 steel in carbonate/bicarbonate solution are needed at potentials in the active, active-to-passive and passive regions to answer this question.

It is possible to evaluate the mechanical properties of films by measuring the mechanical admittance as a function of applied stress and mean stress amplitude in the elastic region. Such measurements would be extremely valuable since almost no data exist concerning the mechanical properties of protective films such as passive layers on ferrous materials and the oxide films on Al alloys. The strain where the film ruptures may be accurately detected as a rapid increase of the mechanical admittance at a certain stress amplitude, which relates directly to strain in the elastic region. Strain rates corresponding to the frequency of the applied stress also play an important role in the stability of surface films. Some enhanced mechanical admittance occurred even in the passive regions at the higher frequencies of applied stress. The mechanical admittance of the C1117 steel in 70°C carbonate/bicarbonate needs to be measured as a function of stress amplitude and frequency in the active, passive and active-to-passive regions to completely evaluate the mechanical properties of the films formed as a function of potential on the steel surface. The results of this study will indicate

the role that the mechanical properties of surface films might have on SCC. Such information is lacking at present.

Preliminary fatigue admittance data related to the CF behavior of Al 7075 are consistent with a slip-band anodic dissolution/oxidation mechanism for CF of the Al 7075 material. The experiments were performed with a constant R ratio of 0.3 and ΔK = 350 Pa$\sqrt{m}$. Further work needs to be performed to evaluate the influences of crack closure by varying the R-ratio over a broader range to include conditions of both nearly complete crack closure and complete crack opening. Also the relationship between fatigue rate and fatigue admittance can be determined from a large number of tests run at different potentials and ΔK. Similar experiments should be performed for steel. Development of a quantitative relationship between fatigue rate and fatigue admittance will provide a rapid means for predicting CF life.

7.0 REFERENCES

1. J.M. Sutclife, R.R. Fessler, W.K. Boyd, R.N. Parkins, Corrosion 28, 313 (1972).

2. R.N. Parkins, N.J.H. Holroyd, Corrosion, 34(8), 253 (1978).

3. N.J.H. Holroyd and R.N. Parkins,Corr. Sci., 20(6), 707 (1980).

4. R.D. Armstrong and A.C. Coates, Corr. Sci., 16, 423 (1976).

5. A.R. Despic, R.G. Raicheff, and J. O'M. Bockris, J. Chem. Phys., 29(2), 926 (1968).

6. T. Pyle, V. Rollins and D. Howard, J.Electrochem Soc. 122, 1445 (1975).

7. G. Demedts and A. P. Van Peteghem, Corros. Sci. 18, 1029 (1978).

8. R.B. Diegle and D.A. Vermilyea, Corrosion 32, 411 (1976).

9. A. Roelandt and J. Vereecken, Surface Technology, 9, 347 (1979).

10. D.E. Talbot, J.W. Martin, C. Chandler and M.I. Sanderson, Metals Technology, 9, 130 (1980).

11. F. Mansfeld and M. Kendig, "Impedance Measurements for the Analysis of Corrosion Induced Failures", Final Report, SC5287.5FR.

12. F. Mansfeld, Corrosion 37, 301 (1981); F. Mansfeld, M.W. Kendig and S. Tsai, Corrosion 38, 570 (1982).

13. H.L. Marcus and G.C. Sih, Engineering Fracture Mechanics, 3, 453 (1971).

14. R.N. Parkins, Metal Science, July 1979, p 381 (1979).

15. D. Duquette, H.H. Uhlig,Trans. ASM 62, 839 (1969).

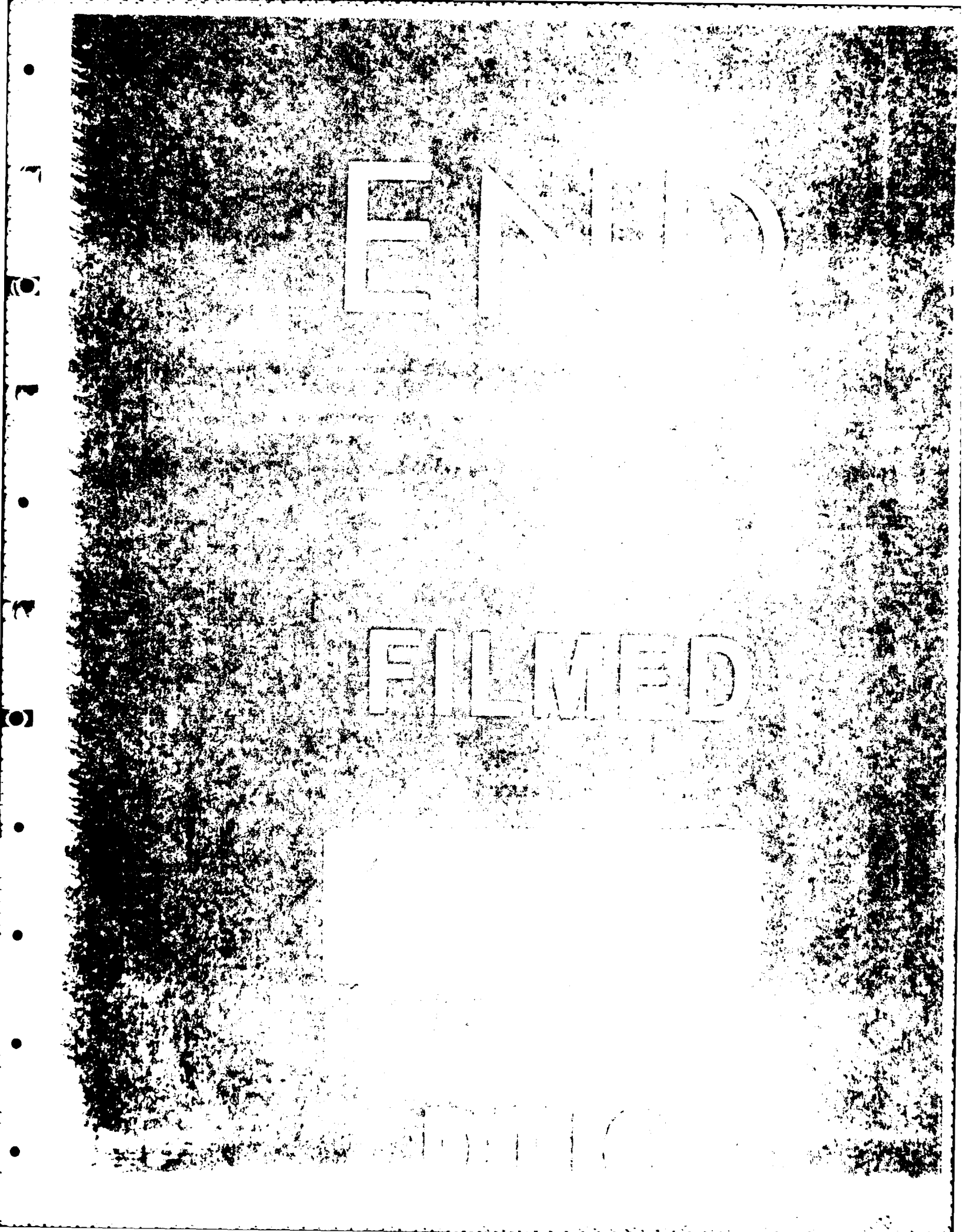
FILMED